# Robot-assisted distal locking of long bone intramedullary nails: localization, registration, and in-vitro experiments

Z. Yaniv and L. Joskowicz

School of Engineering and Computer Science
The Hebrew University of Jerusalem, Jerusalem 91904, Israel.
Email:{zivy,josko}@cs.huji.ac.il

**Abstract.** We are developing an image guided robot-based system to assist orthopaedic surgeons in performing distal locking of long bone intramedullary nails. The system consists of a bone-mounted miniature robot fitted with a drill guide that provides rigid mechanical guidance for hand-held drilling of the distal screws' pilot holes. The robot is automatically positioned so that the drill guide and nail distal locking axes coincide using a single fronto-parallel fluoroscopic X-ray. This paper describes new methods for accurate and robust drill guide and nail hole localization and registration and reports the results of our in-vitro system accuracy experiments. Tests of 17 runs show a mean angular error of $1.3^o$ (std = $0.4^o$) between the computed drill guide axes and the actual locking holes axes, and a mean $3.0mm$ error (std = $1.1mm$) in the entry and exit drill point, which is adequate for successfully locking the nail.

## 1 Introduction

Closed medullary nailing has become the procedure of choice for reducing fractures of the femur and the tibia [2]. It restores the integrity of fractured bone without surgically exposing the fracture with a nail inserted in the medullary canal. The surgeon reduces the fracture by percutaneously manipulating the proximal and distal bone fragments until they are aligned, inserts a guide wire into the medullary canal and drives the nail in. To prevent fragment rotation and bone shortening, the surgeon inserts lateral locking screws. The procedure is performed under X-ray fluoroscopy, which is used to view the position of bone fragments, surgical tools, and implants.

The insertion of the distal interlocking screws is the most challenging step of the procedure. It requires aligning the drill with the nail hole axis by repeatedly imaging the nail and drill with AP and lateral X-rays. Once the drill is aligned, drilling proceeds incrementally, with each advance verified with new images. Complications include inadequate fixation, malrotation, bone cracking, cortical wall penetration, and bone weakening due to multiple or enlarged screw holes. The surgeon's direct exposure to radiation is 3–30 minutes per procedure with 31-51% spent on distal locking alone [11].

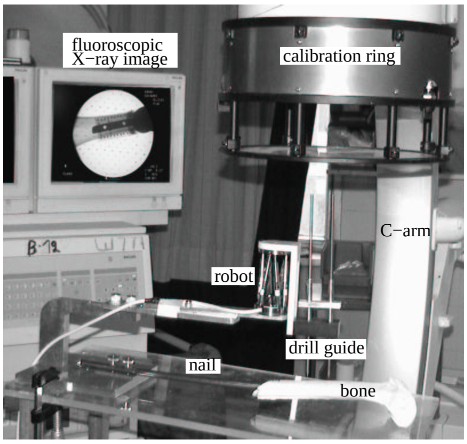


(a) In-vitro setup

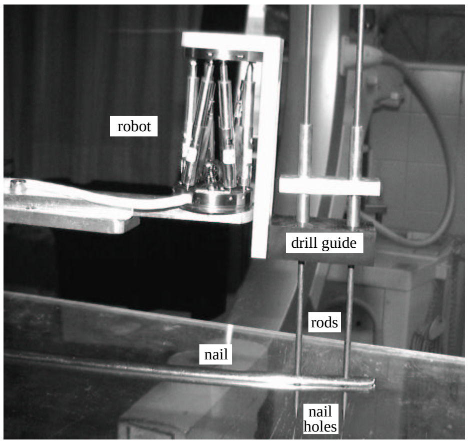


(b) aligned axes configuration

**Fig. 1.** Photographs of (a) the in-vitro setup and (b) the MARS robot in its desired configuration, where the drill guide and nail holes axes are aligned, as shown by the two rods passing through them.

Many devices have been developed for distal locking including proximally mounted targeting devices, mechanical guides, and stereo fluoroscopy [8]. However, all have drawbacks: they are hard to use, are not accurate enough, or cannot always be used. Surgical navigation systems [5] allow the surgeon to position and orient the hand held drill with a few augmented fluoroscopic X-ray images showing in real time the drill position but cannot prevent the drill from slipping or deviating from the desired trajectory.

## 2 System concept

We propose to use the miniature robot MARS [10], originally developed for spinal procedures, to provide mechanical guidance for manual drilling of the holes [6]. MARS is directly mounted on the nail head or on the bone and holds a drill guide whose axes are automatically aligned with the distal nail hole axes based on a single lateral fluoroscopic X-ray image (Fig. 1). Since the robot forms a single rigid body with the bone and the nail, there is no need for leg immobilization or real-time tracking during surgery. To achieve accurate results, the fluoroscopic X-ray C-arm must be calibrated and its images corrected for distortion.

MARS is a 5x5x7$cm^3$, 150–gram 6dof parallel manipulator whose work volume is about 10$cm^3$ and whose accuracy is better than 0.1$mm$. When locked, it is rigid and can withstand forces of a few kilograms. The drill guide is a Delrin block with two guiding holes 30$mm$ apart (the spacing between the nail holes). It has a pattern of 28 3$mm$ stainless steel fiducial spheres asymmetrically placed on two planes 20$mm$ apart that are used for its spatial localization (Fig. 2(a)).

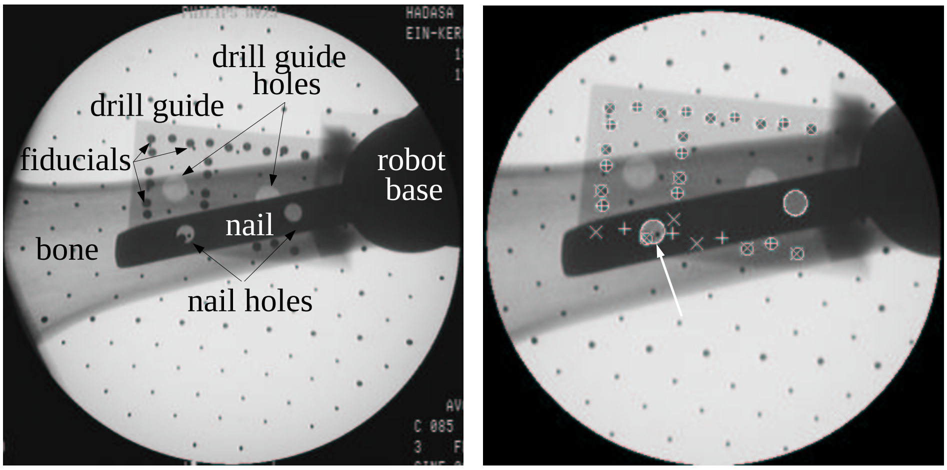


(a) before image processing (b) after localization

**Fig. 2.** (a) Fluoroscopic X-ray image in fronto-parallel setting showing the robot base and drill guide, the nail and its locking holes, and the bone, and; (b) image after distortion correction with detected drill guide pattern and nail holes marked in white. Detected drill guide fiducials are marked as white circles. The fiducials from each of the two target planes are marked as $+$ and $\times$. The arrow indicates the correct detection of drill guide target fiducial and nail hole with partial occlusions.

The surgical protocol is as follows. Once the fracture has been reduced and the nail has been inserted, the surgeon mounts the robot on the nail head or on the bone. The X-ray technician mounts a calibration ring on the C-arm image intensifier and, with the help of a guidance program, orients the C-arm so that it is in a fronto-parallel setting, where the nail holes appear as circles. The localization and registration software automatically determines from the X-ray image the locations of the drill guide and nail holes and computes the robot transformation that aligns their axes. The robot is positioned according to this transformation and locked in place. The surgeon then manually drills the holes and completes the surgery as usual.

## 3 Localization and registration

Accurate and robust computation of the transformation that aligns the drill guide and the nail hole axes is a challenging image processing and pose estimation task. Localization of the nail holes and the drill guide is difficult because partial occlusions are inherent to the setup (the robot is mounted close to the nail holes and the image includes the nail, bone, and soft tissue). The nail holes are small ($5mm$ diameter, about 20 pixels in the image), nearby ($30mm$), and appear as ellipses in the images, so the accuracy with which their axes can be determined is limited. Furthermore, only one fluoroscopic X-ray image can be used, since there

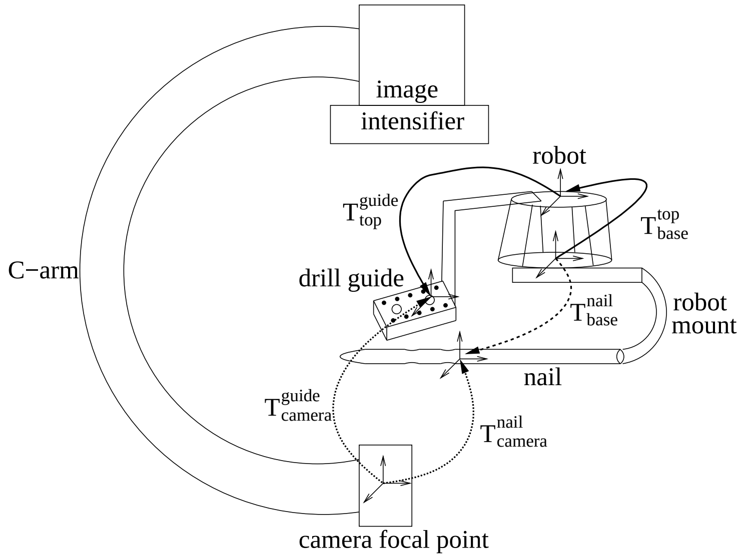


**Fig. 3.** Robot base to nail holes registration chain.

is no tracking of the C-arm pose. Finally, the C-arm imaging system exhibits orientation-dependent distortions and internal imaging parameters variations.

To cope with these challenges, we developed a novel model-based approach for robust and accurate localization of the drill guide target and nail holes and registration of their axes. To facilitate robust nail pose estimation we assume a fronto-parallel setup between nail and C-arm. A nearly perfect fronto-parallel pose can be obtained after a few trials by the X-ray technician with guidance from a program that scores the quality of the pose according to two criteria: hole circularity and the angle between hole supporting plane and the camera viewing direction [7]. When the pose is fronto-parallel, the ellipse aspect ratio is 1 (a circle) and the angle is 0.

We model the fluoroscopic camera as a pin-hole camera with distortion, as this has been shown to be an appropriate approximation of the X-ray. In previous work, we developed a robust automatic C-arm calibration algorithm that includes fiducial localization, distortion correction and camera calibration which achieves an overall submillimetric accuracy even when only 60% of the fiducials are detected [9]. We model the nail as a planar object with two circular holes.

To align the robot so that the drill guide axes coincide with the nail hole axes we compute the transformation between the nail and the robot base, which is given by the following transformation chain (Fig. 3):

$$T_{base}^{nail} = T_{base}^{top} T_{top}^{guide} (T_{camera}^{guide})^{-1} T_{camera}^{nail}$$

where $T_{base}^{top}$ and $T_{top}^{guide}$ are known from design and $T_{camera}^{guide}$ and $T_{camera}^{nail}$ are computed from the C-arm internal camera parameters and the fluoroscopic image.

Our method consists of four steps: 1) C-arm distortion correction and calibration; 2) drill guide identification; 3) nail hole identification; 4) drill guide and nail pose estimation. We describe the later three next.

### 3.1 Drill guide identification

Drill guide identification is performed by first detecting the circular fiducials in the image and then finding the correct correspondence with their 3D model.

The target fiducials are detected in two steps: 1)localization and, 2) circle fitting. Localization is performed using a modified circle Hough transform and a model based analysis of the transform accumulator. As the circular fiducials are darker than their background, we constrain the Hough transform voting scheme so that edge pixels will only cast their vote if the vector connecting them to the hypothesized circle center is in the opposite direction of the gradient at the edge location. Next, the algorithm analyzes the contents of the transform accumulator. Noting that the accumulator may contain multiple peaks for the same fiducial which are greater than the peaks for other fiducials, we examine the $k, k > 28$, circles which received the most votes. Assuming that the five circles with the most votes belong to our target we compute their average radius and number of votes. All circles whose radius is within $\pm 2$ pixels of the average radius and which have received more than half of the average votes are retained. We now have a set of circles which may contain overlapping circles which are either due to multiple responses for the same fiducial or overlapping fiducials. We have empirically observed that for our imaging setup the number of overlapping fiducials is at most two. Utilizing this observation, for each set of overlapping circles we only retain the two circles with the maximal number of votes. These pairs of overlapping circles correspond either to overlapping fiducials or to a single fiducial. This ambiguity is resolved by examining the area of overlap between the pair of circles. If the overlap area is larger than 60% of the circle's area then this is a single circle, otherwise these are two circles.

Circle fitting is performed using the Random Sample Consensus [3] paradigm. For each circle we collect all edge elements contained in its circumscribing square and fit a circle to them. This final step removes the discretization dependent accuracy of the Hough transform.

We now create the correspondence between the detected fiducials and their 3D model using homographies. Directly pairing between the detected fiducials and the 3D model is hard, as there are always missing fiducials, fiducials which are occluded by the nail or failures of our detection algorithm. Using the geometry of the drill guide target to create the correspondence overcomes this problem, instead of points we use lines which are more robust to partial occlusions. As the fiducials are distributed on two planes we seek the pair of homographies which minimizes the distance between the detected circles and the result of applying the homographies to the target fiducials. Finding this pair of homographies is done in three steps: (1) Identify the line which passes through the maximal number of detected circles. This line is one of the pattern axes. (2) Find all lines which are parallel/perpendicular (within a range of $\pm 5^o$) to this line and that pass only through two circles. The target is built such that the two spheres on these lines are on the same plane. (3) This set of lines defines a discrete and small set of possible line matches between image and target lines. Try all possible matches and find the best one. Finally, using the optimal pair of homographies we map the target fiducials to the image and identify the detected circles accordingly (Fig. 2(b)).

### 3.2 Nail hole identification

The distal locking nail holes location in the fluoroscopic X-ray image is determined by first locating the nail's longitudinal contour and then locating its holes from their expected position with respect to this contour. To locate the nail longitudinal contours, we apply a Canny edge detector followed by a 3D Hough transform in which the nail is modeled as a band consisting of two parallel lines at a known distance between them. The Hough transform voting scheme is constrained so that pixels which are on parallel lines will only cast their vote if the gray level values between them are lower than the gray level values outside the band. All the pixels outside the contours are discarded.

The search for the nail holes is then performed on the pixels contained between the nail's contours, since the nail holes lie between these two lines. The algorithm sweeps a parallelepiped window whose sizes are equal to the nail width along the nail's medial axis. The two locations containing the maximal number of edge elements correspond to the locations of the distal locking nail holes.

We now fit an ellipse to the edge data contained inside the parallelepipeds. These edge elements originate from the nail holes, the drill guide target and the C-arm calibration target (Fig. 2(b)). The ellipse parameter estimation is performed by only using edge elements which belong to the convex hull of the set of elements we found. This is based on the following two facts: outlying edges can only be present in the interior of the ellipse, as nothing is visible through the nail, and ellipses are convex shapes. We then fit an ellipse to the edge elements using a non-linear geometric least squares method initialized with the estimate computed using an algebraic least squares method [4].

### 3.3 Drill guide and nail pose estimation

The drill guide pose is computed by non-linear minimization of the projection distances between the known fiducial projection coordinates $(x_i, y_i)$ and the expected ones $(\widehat{x_i}, \widehat{y_i})$:

$$\mathbf{v}^* = \arg\min_{\mathbf{v}} 0.5 \left( \sum_{i=1}^{n} (x_i - \widehat{x_i}(\mathbf{v}))^2 + (y_i - \widehat{y_i}(\mathbf{v}))^2 \right)$$

where $\mathbf{v}$ is the rigid transformation parameterization. The solution is found using the Levenberg-Marquardt method with an initial estimate obtained with the linear method described in [1].

The nail pose is computed using the fronto-parallel setup assumption, the projective transformation applied to the nail holes has degenerated to a similarity. The computation is done directly from the nail holes coordinates in the image, $(\mathbf{p}_x, \mathbf{p}_y)$ and $(\mathbf{q}_x, \mathbf{q}_y)$, their average diameter on the image $d_{im}$, their real diameter $d$, and the camera focal length $f$. The nail location is:

$$\mathbf{t} = \begin{bmatrix} \frac{z}{f}\mathbf{p}_x \\ \frac{z}{f}\mathbf{p}_y \\ z \end{bmatrix}$$

where $z = fd/d_{im}$ is the nail distance from the camera focal point. The nail orientation relative to the camera is:

$$R = \begin{bmatrix} \mathbf{p}_x - \mathbf{q}_x & \mathbf{p}_y - \mathbf{q}_y & 0 \\ \mathbf{p}_y - \mathbf{q}_y & \mathbf{q}_x - \mathbf{p}_x & 0 \\ 0 & 0 & -1 \end{bmatrix}$$

The nail's $X$ axis direction, which depends on the order in which $(\mathbf{p}, \mathbf{q})$ are chosen, is set so that its angular deviation from the direction of the drill guide's $X$ axis is minimal.

## 4 Experimental results

We conducted three sets of experiments to quantify the accuracy and robustness of the proposed method. To test the robustness of the drill guide and nail hole identification, we manually placed the robot and C-arm in random positions. We then acquired 67 fluoroscopic X-ray images. The drill guide and nail holes were correctly identified in 61 images. There were no false positives, i.e., the detection was correct in all images for which our software stated that the drill guide and nail holes were detected. All six failures were automatically detected by the software. They were caused by occlusion of many drill guide target fiducials, which prevented its proper localization.

To quantify the accuracy of the whole system for the task at hand, we define two error measures: the angular deviation of the drill guide axes and the distance between axes entry and exit points, which is the in-plane distance between the intersection points of the axes and two planes located at $100mm$ and $120mm$ from the robot base (the nail is located between these planes).

We then conducted the following experiment. The robot was first manually placed in a pose in which two $4mm$ diameter cylindrical rods with tapered ends pass through the $5mm$ diameter drill guide and nail holes as shown in Fig. 1(b). This pose guarantees successful locking and constitutes the robot's reference pose. To quantify the variability of the reference poses, we placed the robot in 17 different poses in which the two rods passed through the drill guide and nail holes and computed the two error measures. We found an angular variation of $0^o - 0.9^o$ and a translational variation in the entry and exit points of $0 - 3.9mm$. This means that a registration accuracy of about $1^o$ and $\pm 2mm$ will guarantee successful distal locking.

Next, under the guidance of our software, we oriented the C-arm so that it formed a fronto-parallel setup with the nail holes. We placed the robot in 17 random poses, acquired fluoroscopic X-ray images for each pose, and computed the robot alignment transformation for each pose (in all cases, the drill guide target and nail holes were correctly detected). Comparing the 17 computed robot poses to the reference pose our results show a mean angular error of $1.3^o$ (std = $0.4^o$) between drill guide axes, and a mean $3.0mm$ error (std = $1.1mm$) in the entry and exit points, which is adequate for successfully locking the nail.

## 5 Conclusions

We have presented a robust, automatic method for aligning the drill guide and the nail holes axes based on a few fluoroscopic X-ray images. The method is part of a new image-guided miniature robot-based system to assist orthopaedic surgeons in performing distal locking of long bone intramedullary nails. Our experimental results show that the automatic localization is feasible within the required accuracy. We are currently working on mechanical and algorithmic improvements to increase the accuracy of the system, and will then proceed with a cadaver and in-vivo evaluation.

## References


1. Ansar A., Daniilidis K., "Linear pose estimation from points or lines", *IEEE Trans. on Pattern Analysis and Machine Intelligence*, **25**(5), 2003.
2. Brumback R.J., "Regular and special features – the rationales of interlocking nailing of the femur, tibia, and humerus", *Clinical Orthopaedics*, **324**, 1996.
3. Fischler M. A., Bolles R. C., "Random sample consensus: a paradigm for model fitting with applications to image analysis and automated cartography", *Communications of the ACM*, **24**(6), 1981.
4. Fitzgibbon A., Pilu M., Fisher R. B., "Direct least square fitting of ellipses", *IEEE Trans. on Pattern Analysis and Machine Intelligence*, **21**(5), 1999.
5. Joskowicz L., Hazan E., "Computer-assisted image-guided intramedullary nailing surgery of femoral fractures" (in French), *Monographie des Conferences d'Enseignement de la SOFTCOT*, Vol. 80, Elsevier, 2003.
6. Joskowicz, L., Milgrom, C., Shoham, M., Yaniv, Z., Simkin, A., "A robot-assisted system for long bone intramedullary distal locking: concept and preliminary results", *Proc. of the 17th Int. Congress on Computer-Assisted Radiology and Surgery*, CARS'2003, H.U. Lemke *et. al.* editors, Elsevier 2003, pp 485–491.
7. Kanatani K., Liu W., "3D interpretation of conics and orthogonality", *Image Understanding*, **58**(3), 1993.
8. Krettek C. et al., "A mechanical distal aiming device for distal locking in femoral nails", *Clinical Orthopaedics*, **384**, 1999.
9. Livyatan H., Yaniv Z., Joskowicz L., "Robust automatic C-arm calibration for fluoroscopy-based navigation: a practical approach", *Proc. of Medical Image Computing and Computer Assisted Intervention*, 2002.
10. Shoham, M., Burman, M., Zehavi, E., Joskowicz, L., Batkikin, E., Kunicher, Y., "Bone-mounted miniature robot for surgical procedures: concept and clinical applications", *IEEE Trans. on Robotics and Automation*, **19**(5), 2003.

11. Skejdal S., Backe S., "Interlocking medullary nails - radiation doses in distal targeting", *Archives of Orthopaedic Trauma Surgery*, **106**, 1987.